Thin-Walled Structures 137 (2019) 271–283

Contents lists available at ScienceDirect

Thin-Walled Structures

journal homepage: www.elsevier.com/locate/tws

Full length article

A comparative study on tensile behavior of welded T-stub joints using Q345 normal steel and Q690 high strength steel under bolt preloading cases

Gang Liang[a,b], Hongchao Guo[a,b], Yunhe Liu[a,b,*], Dixiong Yang[a,b], Shen Li[a,b]

[a] State Key Laboratory of Eco-hydraulics in Northwest Arid Region of China, Xi'an University of Technology, No.5 Jinhua Road, Xi'an 710048, PR China
[b] School of Civil Engineering and Architecture, Xi'an University of Technology, No.5 Jinhua Road, Xi'an, Shaanxi Province 710048, PR China

ARTICLE INFO

Keywords:
High strength steel
Bolt preloading
Failure mode
Bearing capacity
Ductility index
Faella stiffness formulation
EC3 code

ABSTRACT

To reveal more information and understand the difference in failure mechanisms and mechanical behaviors of welded T-stub joints with different steel grades under bolt preloading cases, a systematic experimental study was conducted in this paper. The tensile performance of the welded T-stub joint with Q690 high strength steel (HSS) and Q345 normal steel (NS) was compared and evaluated. Especially, the properties of stiffness, resistance and ductility varying with the bolt diameter, strength grade and the ratio of bolt edge distance e to bolt distance d from the web. Moreover, the Faella stiffness formulations and the provisions of Eurocode 3 Part 1–8 were validated against the test results of HSS welded T-stub joints. It was found that, the failure of only the flange occurred near the weld toe can ensure a good ductility for the welded T-stub joints with NS, but for HSS welded T-stub joints there is still a brittle rupture mode due to little necking developed. The plastic resistance of welded T-stub joints with HSS is higher than that of those joints using NS by about 24–66%, while its ultimate bearing capacity is slightly more than that of those joints with NS by around 1–23%. The empirical stiffness coefficient ψ in Faella stiffness formulation significantly overestimates the bolt restraining action of the HSS welded T-stub joints. In addition, EC3 resistance equations may be not safe to predict the actual resistance of the HSS welded T-stub joints when the flange fracture near the weld toe governs the collapse, due to the influence of welding process.

1. Introduction

Owing to the substantial advantages in architectural style, structural safety and economic benefit [1–4], high strength steel (HSS, yield strength $f_y \geq 460$ MPa) has been increasingly applied in high-rise buildings, large span bridges and space structures in the past two decades [5]. However, the market share that HSS holds does not reflect its competitiveness because of the lack of necessary researches on welded or bolted joints with HSS. Compared with the normal steel (NS), the yield ratio of HSS increases with the increasing steel grade, while its elastic modulus remains unchanged, and even the elongation at fracture, the toughness, and ductility will decrease [6]. Hence, the difference in mechanical properties between HSS and NS joints need to be examined elaborately.

However, nowadays, only limited research results on the HSS connection joints were reported in literature. Sun et al. [7] analyzed the mechanical behavior of flush endplate connections made of Q690 HSS and Q345 NS. It is found that HSS endplate connection has obvious advantages in bending bearing capacity, but the bolts are prone to failure before the yield of endplate, and it is suggested to use the large size bolts to improve the ductility of HSS endplate connection. Coelho et al. [8] performed an experimental study on the mechanical behavior of end-plate connections using S690 HSS under monotonic tensile load, and it is observed that the rotation bearing capacity of HSS joint meets relatively the high requirements of deformation. Qiang et al. [9,10] carried out an experimental and numerical study on the behavior of beam-to-column HSS endplate connections under fire condition, and it is showed that compared with the connections using thick NS endplate, a relatively thin HSS endplate can present the same failure mode, similar load bearing capacity and the comparable or even higher rotation capacity. Jordão et al. [11] conducted a contrastive analysis on welded beam-to-column joints using S355 NS and S690 HSS, and analyzed the effectiveness of Eurocode 3 Part: 1–8 (EC3) [12] component method for predicting the stiffness and resistance of the HSS column-web panels. Zhao et al. [13–15] simply considered the effect of the flange thickness on tensile behavior of T-stub joints using S690 HSS, S385 and S440 NS,

* Corresponding author at: School of Civil Engineering and Architecture, Xi'an University of Technology, No.5 Jinhua Road, Xi'an City, Shaanxi Province 710048, PR China.
E-mail addresses: lg20854007@163.com (G. Liang), liuyunhe1968@163.com (Y. Liu).

https://doi.org/10.1016/j.tws.2019.01.023
Received 27 July 2018; Received in revised form 28 October 2018; Accepted 11 January 2019

and their research results indicate that the plastic resistances of the T-stub joints with S690 HSS are generally lower than the predicted values by both the yield line method and the EC3 equations, due to the strength reduction of the plastic hinges near the weld toe of the T-stub joint. This point implies that HSS joint has major difference compared with NS joint around the weld toe, because the mechanical change is induced by welding process. Noted that the effect of bolt preloading on the mechanical behavior of HSS T-stub joints is not considered in the above literature. In some cases, beam-to-column bolted joints need to be preloaded in order to bear the fatigue loads or even just to increase the connection stiffness [16,17]. The preloading modifies the overall behavior of the T-stub joint, affecting both the flange span and the boundary conditions. Faella et al. [18] studied these phenomena and proposed a methodology based on an empirical stiffness coefficient ψ, which depends on the flange thickness, the bolt diameter, and the geometrical parameter m of T-stub joint. This coefficient modifies the stiffness of the cantilever approach in the intermediate cases between very thick and very thin T-stub flanges, i.e. the pinned and the fixed cases, respectively. Liang et al. [19] and Guo et al. [20] carried out an experimental and numerical analysis of mechanical properties of Q690 HSS T-stub joints with bolt preloading, and analyzed theoretically the difference of the initial stiffness between HSS and NS T-stub joints, but lack of effective test verification. Coelho et al. [21] examined the effect of the key parameters on the mechanical properties of NS T-stub joints, which indicated that apart from the parameters including bolt diameter, strength grade and flange thickness, the steel grade has great influence on the mechanical properties of connection joints. Hence, more influence parameters should be taken into account to analyze the mechanical performance of HSS and NS T-stub joints, especially for those joints with bolt preloading.

The aim of this work is to reveal more information and understand the difference in mechanical behaviors of welded T-stub joints using Q690 (HSS, the nominal yield stress of which is 690 MPa, similar to S690 steel defined by Eurocode 3 Part 1–12 [22]) and Q345 (NS, the nominal yield stress of which is 345 MPa, similar to S355 steel defined by Eurocode 3 Part 1–12 [22]) by both experimental and theoretical methods. In the experimental study phase, 10 HSS specimens and 10 NS specimens were fabricated and tested separately. The failure mode, load-displacement behavior, initial stiffness, plastic resistance, ultimate bearing capacity and ductility index of the HSS T-stub joints were obtained through tests and compared with those of NS T-stub joints. In the theoretical phase, the provisions of EC3 [12] and the stiffness formulations proposed by Faella et al. [18] were validated with a series of test results of HSS T-stub joints with bolt preloading. This experimental study makes a certain contribution in paving a way for the engineering application of HSS structure to substitute for NS structure.

2. Experimental program of welded T-stub joints

2.1. Specimen fabrication

In this type of T-stub assembly, two plates, web and flange with same steel grade were welded together by means of double groove butt weld according to the *code for welding of steel structures* (GB 50661–2011) [23], in which the employed electrodes for Q690 and Q345 steel are CHE857cr and E50 types respectively, and the weld grades are Grade I. The configuration of a single T-stub element is shown in Fig. 1, where one bolt hole was drilled at each side of the chord plate in order to study the effect of bolt specification. Herein, twenty welded T-stub joints, with web thickness t_w of 10 mm, and flange width b of 100 mm, were fabricated by using the Q690 HSS and Q345 NS plates. The distinction among T-stubs lies in the bolt specification and geometry, the dimensions adopted for each steel grade are displayed in Table 1, and the specimens in Table 1 are distinguished by the key parameters. The diameters and strength grades of bolts between group 1 and group 2 are different, and the ratio of bolt edge distance e to bolt distance d from the web is varied in group 3. In addition, Table 1 also implies that the specification and size of HSS T-stub joints in all specimens are equal to those of NS joints to facilitate the comparison of mechanical behaviors. The consistence between HSS and NS specimens can be ensured by measuring the actual size and arrangement before and after the welding. For easy reference, each specimen is assigned a test code. The term 'WT' and 'HWT' refers to specimens with welded T-stub joints using Q345 NS and Q690 HSS, respectively, and the numbers following the capital letter stand for the order of the specimens.

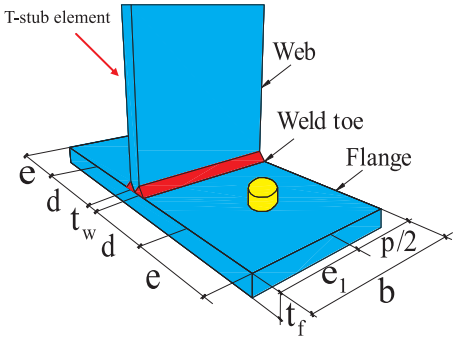

Fig. 1. Geometry characteristics of single T-stub element.

In the Eurocode 3 Part 1–1 [24], to prevent non-ductile failure of endplate connection with NS, the thickness of the endplate should be limited within 60% of the bolt diameter. Moreover, the Eurocode 3 Part 1–8 [12] set the following values for T-stub joints: $n = e$, $m = d–0.8\,s$, $n/m \leq 1.25$, where s denotes the fillet weld size, and the variables e and d are illustrated in Fig. 1. A 10 mm thick flange plate using Q690 HSS and Q345 NS is employed in this study. The HWT1/WT1 and HWT4/WT4 specimens with M16 bolt diameter, the HWT9/WT9 and HWT10/WT10 specimens with e/d of 1.5 and 1.75 respectively are designed to investigate the extreme case; the remaining specimens are designed to represent the commonly-used T-stub sizes.

2.2. Material properties

The material property test was conducted under relevant regulations in the *Metallic materials—Tensile testing—Part 1: Method of test at room temperature* (GB/T228.1–2010) [25] and *Steel and steel products—Location and preparation of test pieces for mechanical testing* (GB/T2975-1998) [26]. Three tensile coupon tests for each original plate and a total of 6 tensile coupon tests were carried out. The average values of mechanical properties of the 3 tensile coupons for each steel grade are listed in Table 2. In Table 2, f_y means the yield strength of the steel plates, f_u denotes the ultimate tensile stress, E indicates elastic modulus. Note that, unlike NSs, tensile stress-strain curves for Q690 HSSs did not exhibit an obvious yield plateau. Thus, the proof stress corresponding to 0.2% residual plastic strain was treated as yield strength. Moreover, the tensile coupons for Q690 HSS is of superior bearing capacity, and its yield stress and ultimate stress is 82% and 39% higher than that of Q345 NS respectively, while the elongation after fracture is only about half of that of Q345 NS, as shown in Fig. 2. The strengths of the same batches of bolts in Table 3 are given by a specialized quality inspection institution.

2.3. Test setup and measurement

The T-stub joint is consisted of two T-shaped elements connected through the flanges by means of one or more bolt rows [27]. To avoid the influence of bolt group effect on mechanical properties of these joints, only one bolt row is employed in this study. The bolt preloading level is determined by the provisions of *Technical specification for high strength bolt connections of steel structures* (JGJ82–2011) [28]. The construction pretension force P_c of high-strength bolt are illustrated in

Table 1
Design parameters of specimens.

Group number	Specimen code		T-stub geometrical sizes (mm)							Bolt characteristics
			t_f	t_w	e_1	$p/2$	e	d	e/d	
1.	HWT1	WT1	10	10	46	54	50	50	1.0	M16, 8.8 *s*
	HWT2	WT2	10	10	46	54	50	50	1.0	M20, 8.8 *s*
	HWT3	WT3	10	10	46	54	50	50	1.0	M24, 8.8 *s*
2.	HWT4	WT4	10	10	46	54	50	50	1.0	M16, 10.9 *s*
	HWT5	WT5	10	10	46	54	50	50	1.0	M20, 10.9 *s*
	HWT6	WT6	10	10	46	54	50	50	1.0	M24, 10.9 *s*
3.	HWT7	WT7	10	10	46	54	50	67	0.75	M20, 8.8 *s*
	HWT8	WT8	10	10	46	54	50	100	0.50	M20, 8.8 *s*
	HWT9	WT9	10	10	46	54	75	50	1.50	M20, 8.8 *s*
	HWT10	WT10	10	10	46	54	87.5	50	1.75	M20, 8.8 *s*

Note that the term 'WT' and 'HWT' refers to specimens with welded T-stub joints made of Q345 NS and Q690 HSS respectively, and the numbers following the capital letter stand for the order of the specimens.

Table 2
Mechanical properties of the steels.

Steel grade	Thickness t (mm)	Elastic modulus E (10^5 MPa)	Yield stress f_y (MPa)	Ultimate stress f_u (MPa)	Elongation after fracture (%)
Q345B	10	1.93	417.60	564.86	31.03
GB/T1591–2008 Q345 t ≤ 16 mm			≥ 345	470–630	≥ 20
Q690D	10	2.09	760.93	784.08	15.27
GB/T1591–2008 Q690 t ≤ 16 mm			≥ 690	770–940	≥ 14

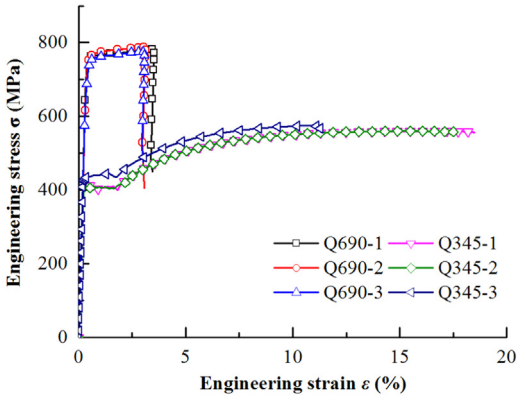

Fig. 2. Stress-strain curves.

Table 3
Mechanical properties of high-strength bolts.

Bolt grade	Yield stress $f_{y,b}$ (MPa)	Ultimate stress $f_{u,b}$ (MPa)
8.8 *s*	833	947
10.9 *s*	995	1100

Table 4
Construction pretension force of high-strength bolts (in kN).

Bolt grade	Bolt specification		
	M16	M20	M24
8.8 *s*	90	140	195
10.9 *s*	110	170	250

Table 4.

The preloading force on the high-strength bolts are applied by the torque wrench, and further the relationship between the final construction torque T_c and P_c has been provided

$$T_c = kP_cd_b \quad (1)$$

where d_b is bolt diameter; k is the average value of torque-pretension coefficient, k = 0.11–0.15, herein the coefficient k is taken as 0.15 and then the value T_c applied on the high-strength bolts can be eventually obtained by Eq. (1).

Fig. 3 illustrates the general arrangement of the test setup. Both ends of specimen are fixed on the MTS hydraulic clamp with a clamping force of 28 MPa. The vertical load is applied by a 100 t MTS actuator. The displacement in the centreline of the webs is measured with two linear variable displacement transducers (LVDTs), and eventually taking the average value measured by the two LVDTs as the displacement of each specimen [27]. The displacement and strain data are collected through Data Logger TDS-303. The loading procedure of the tensile test goes through 3 phases. In the first two phases, the loading is controlled by force, and in the third phase, the loading is controlled by force before the specimen yields and thereafter by displacement. In the first phase, applying load reaches to (2/3) $F_{Rd,0}$, which corresponds to the theoretical elastic limit. $F_{Rd,0}$ indicates the plastic resistance and is calculated according to EC3 [12]. In the second phase, unloading drops from (2/3) $F_{Rd,0}$ to zero. In the third phase, the specimen is reloaded up to failure. The force control's speed is 0.5 – 2 kN/s and the displacement control's speed is 0.04 mm/s [19,20]. The loading is stopped in either of the following cases: (1) specimen failure, including the flange fracture or bolt failure; (2) the bearing capacity of specimen drops to 85% peak load.

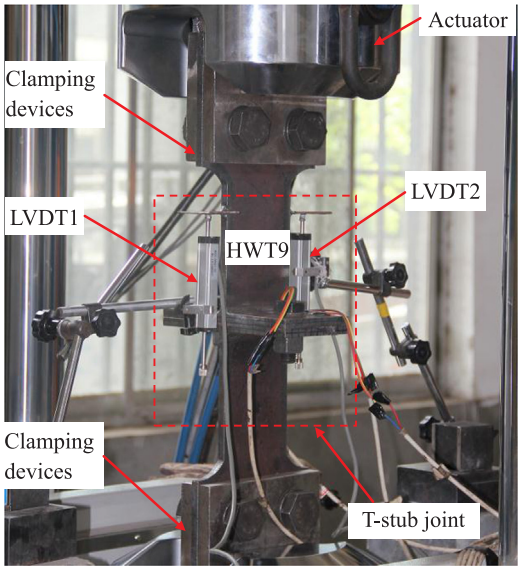

Fig. 3. Test setup.

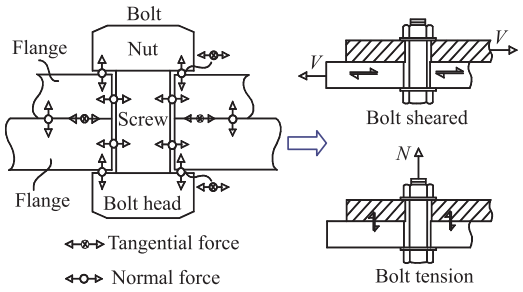

Fig. 4. Interaction mechanism between the bolt and the flange.

3. Test results and analysis for T-stub joints

3.1. Failure modes

The interaction mechanism between the bolt and flange of T-stub joint in tension is shown in Fig. 4. Their compression each other results in the bending and shear deformation of the bolt shank and hole wall respectively. The deformation capacity of T-stub joint made up of welded plates primarily depends on the plate/bolt strength ratio and the weld resistance [27].

To analyze qualitatively the distinction in the breakdown characteristics, the failure modes of the T-stub joints utilizing HSS and NS respectively are compared and discussed herein. In Group 1, the specimen WT1 failed in a mixed mode, the collapse of which was determined by bolt fracture with some damage of the plate near the weld toe as well, while the specimen HWT1 presented a stripping phenomenon of the nut threads. The distinction between them is that the latter has no cracks of the plate occurred near the weld toe, as clearly illustrated in Fig. 5a and b. The flange fracture occurred merely near the weld toe was observed in the specimens WT2 and HWT2, as well as the specimens WT3 and HWT3, the residual deformation after collapse is illustrated in Fig. 5c and d, e and f respectively. Notice that for the specimen with NS (normal steel), the excellent plastic deformability was confirmed by this research, as evidenced by some phenomena including the apparent necking after the flange fracture near the weld toe, the concave around the bolt and the indentation on the flange etc. However, for the specimens with HSS (high strength steel), a brittle rupture mode occurred near the weld toe because of little necking developed (see Fig. 5d and f), which further implied that the plastic deformability of the T-stub joints using HSS is much smaller than that of those NS joints, and the former develops small bending deformation in the flange. The failure mode of the specimens WT4 and HWT4 in Group 2 is also a mixed mode, and their residual deformations are compared in Fig. 5g and h. After collapse, the bolt hole became ellipse due to the interaction between the flange and bolt (see Fig. 5g), and meanwhile small bending deformation for HWT4 was expected when compared to the test WT4. The welds connecting the flange and web cracked under the tension load, due to the possible welding defects in specimen WT5. Fig. 5i demonstrates the specimens in failure condition, it must be pointed out that the weld fracture is not expected in actual application. Unlike the specimen WT5, the flange fracture with little plastic deformation near the weld toe again appeared in specimen HWT5, as can be seen from Fig. 5j. The failure mode of the specimen WT6 is a good consistence with that of the specimen HWT6, but they are different in plastic deformation, as shown in Fig. 5k and l. In Group 3, the weld fracture and flange fracture near the weld toe were found in the specimens WT7 and HWT7 respectively, as indicated in Fig. 5m and n. The largest flange span is arranged in the specimens WT8 and HWT8 herein. As can be seen from Fig. 5o and p, the excessive bending deformation occurred in specimen WT8. Unfortunately, due to the maximum displacement limit of the MTS, the ultimate breakdown case was not observed in the specimen WT8, while the specimen HWT8 damaged in a flange fracture with some bending deformation. The breakdown characteristics of the remaining specimens WT9 and HWT9, WT10 and HWT10, are respectively compared in Fig. 5q and r, s and t. Under ultimate condition, due to the larger bending deformation developed in the specimens using NS, the high strength bolts in NS specimens bear greater external load than these in specimens made of HSS according to the test records. Therefore, the bolt failure was observed in the specimens WT9 and WT10, while only flange fracture near the weld toe appeared in specimens HTW9 and HWT10.

In summary, the failure modes of the T-stub joints with high grade steel are basically the same as those of joints with low grade steel. Fracture of the bolts or the welds presents a brittle rupture mode, and only the failure of flange occurred near the weld toe can ensure a good ductility for the NS welded T-stub joints, but for HSS welded T-stub joints there is still a brittle rupture mode due to little necking developed.

3.2. Load-displacement characteristic

The most significant characteristic describing the overall behavior of the T-stub joints is the load-deformation (F–△ for short) response. Fig. 6 compares the F–△ results for the HSS and NS welded T-stub joints respectively, with different bolt diameters, strength grades and e/d ratios. It is shown that for the NS T-stub joints, the F–△ curves are smooth before failure, and the deformation of the specimens increases continuously during the loading, which again indicates that the specimen using NS possesses obvious advantage of plastic deformation. However, for those joints using HSS, a load oscillation case is observed in the F–△curves, resulting from the local rupture of the flange near the weld toe, which means that HSS welded connections have apparent brittle fracture characteristic in tension. The effect of the bolt diameters on the whole response is depicted in Fig. 6a and b. if the deformation capacity of the joint is evaluated at the maximum deformation level, Fig. 6a clearly shows that if the bolt diameter increases, the strength and the deformation level of both HSS and NS T-stubs also increase, because a large restraint is introduced on the flange and improves the bearing capacity, the deformation is mainly the flange bending deformation with good ductility, when compared to the deformation of the high-strength bolts. Nevertheless, for the specimens with HSS, the opposite phenomenon for the deformation capacity is observed in Fig. 6b, which depends on the effect of plastic deformability and effective span of the flange. Fig. 6a and b also illustrate that decreasing the bolt strength grade, the deformation capacity of the joints using HSS does not increase obviously.

Apart from the bolt type, influence of the parameter e/d ratio on tensile behavior of the joints should not be ignored. As shown in Fig. 6c, the bearing capacity of these joints using HSS and NS increases as the e/d ratio increases, while their deformation capacity decreases. Due to decreasing effective span of the flange. Surprisingly, when the $e/d \geq 1.5$, the F–△ response of the specimen WT9 is almost coincided with that of WT10. But for HSS joints, before the load oscillation case occurred, identical situation was observed in HWT9 and HWT10. Thereafter, the failure happened prematurely in the specimen HWT10 due to fracture of the flange near the weld toe, the ultimate bearing capacity between them is nearly the same, while the deformation level of HWT9 is greater than that of HWT10. Thus, the conclusions can be drawn that, for the ultimate bearing capacity and deformation level of the specimens, the maximum value of the NS specimens were obtained when the e/d ratio was 1.5 and 1.0 respectively. While for the HSS specimens, they were achieved at $e/d = 1.5$.

To quantitatively compare and analyze the initial stiffness, plastic resistance, ultimate bearing capacity and ductility of these joints using those two materials, the F–△ curves are simplified as a bilinear function [8,29], and thus the main characteristic value in this case can be obtained by the methods shown in Fig. 7. In Fig. 7, the notations are further explained as follows [29]:

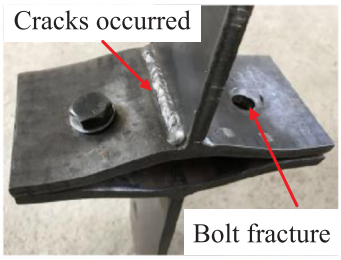

(a) Specimen WT1, a mixed mode

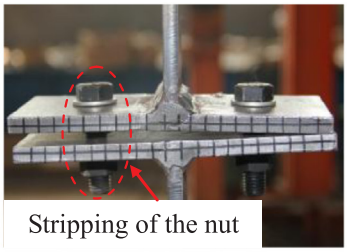

(b) Specimen HWT1, stripping of the nut threads

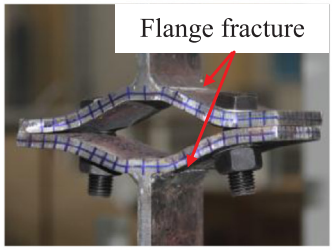

(c) Specimen WT2, flange fracture

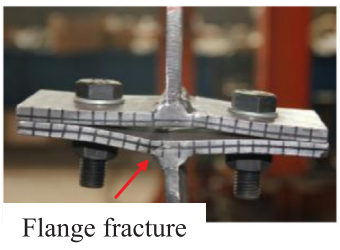

(d) Specimen HWT2, flange fracture

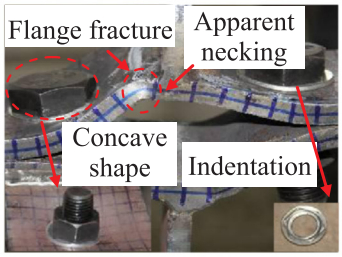

(e) Specimen WT3, flange fracture

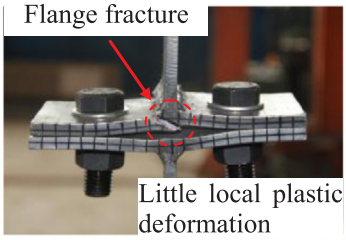

(f) Specimen HWT3, flange fracture

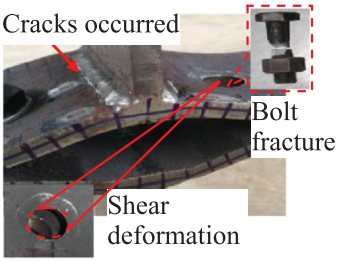

(g) Specimen WT4, a mixed mode

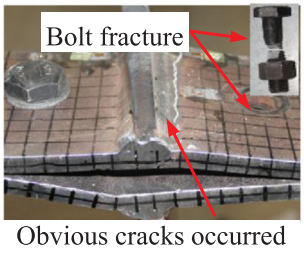

(h) Specimen HWT4, a mixed mode

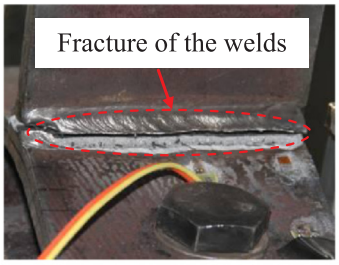

(i) Specimen WT5, weld fracture

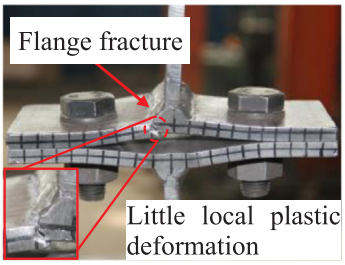

(j) Specimen HWT5, flange fracture

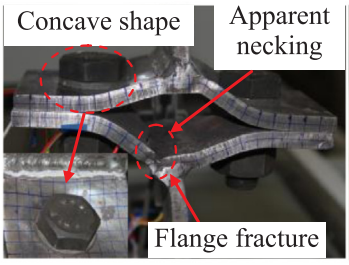

(k) Specimen WT6, flange fracture

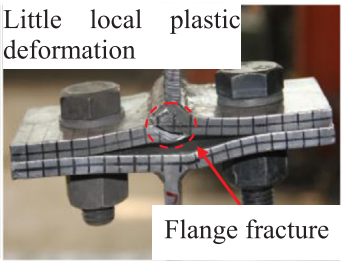

(l) Specimen HWT6, flange fracture

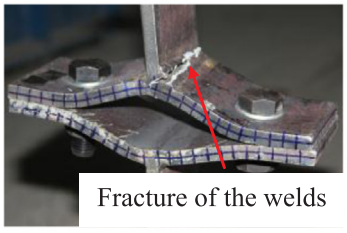

(m) Specimen WT7, weld fracture

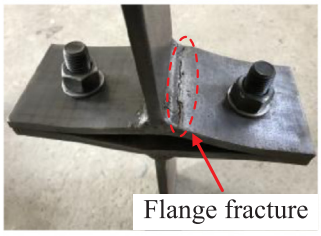

(n) Specimen HWT7, flange fracture

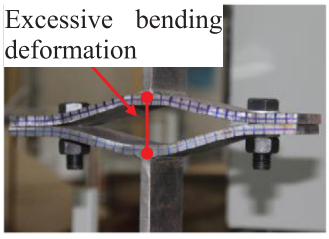

(o) Specimen WT8, no failure

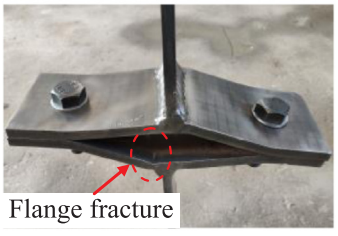

(p) Specimen HWT8, flange fracture

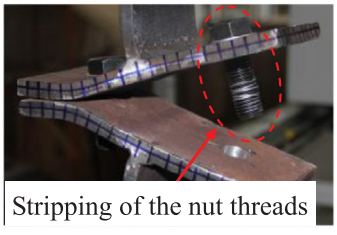

(q) Specimen WT9, stripping of the nut threads

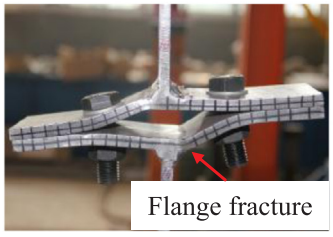

(r) Specimen HWT9, flange fracture

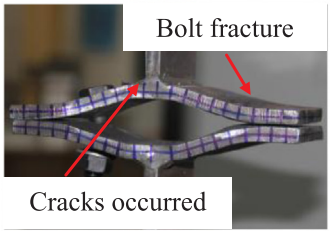

(s) Specimen WT10, a mixed mode

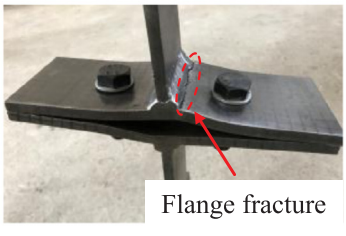

(t) Specimen HWT10, flange fracture

Fig. 5. Failure modes.

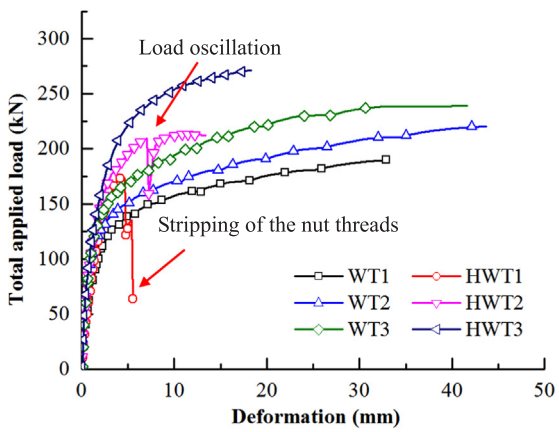

(a) The effect of grade 8.8*s* bolts

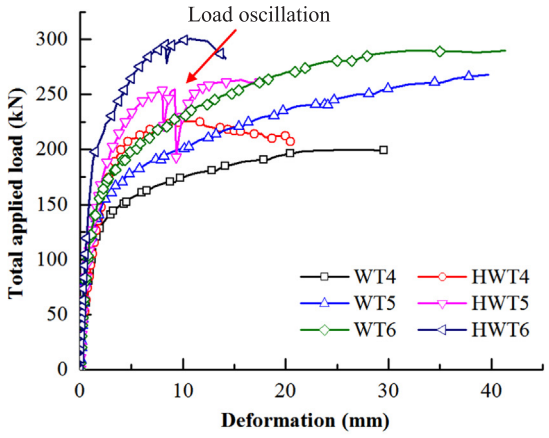

(b) The effect of grade 10.9*s* bolts

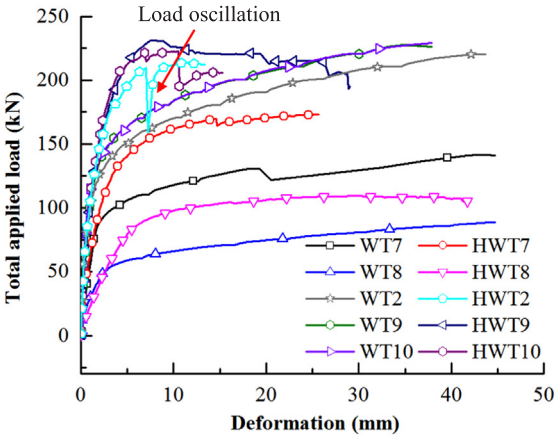

(c) The effect of *e*/*d* ratio

Fig. 6. Load-deformation curves.

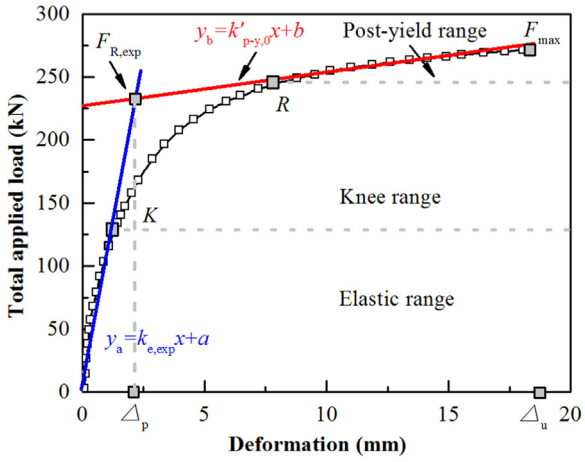

Fig. 7. The key points of load-displacement curves.

K–*R* – knee range *K*–*R* (corresponds to the transition from the stiff (elastic) to the soft (post-yield) part; *K* is the lower bond and *R* is the upper bound of the knee-range);
$k_{e,exp}$ – experimental elastic stiffness computed by means of a regression analysis of the unloading portion of the *F*–Δ curve (which is not traced in the graphs);
$k_{p-y,0}$ – post-yield stiffness, the slope of the line which is obtained by the linear regression analysis of the *F*–Δ curve in the post-yield range after *K*–*R* till failure;
$F_{R,exp}$ – plastic resistance obtained at the crossing point of the line passing by the point *K* and the line which represents the post-yield range, namely y_b;
F_{max} – ultimate (maximal) bearing capacity;
Δ_p – yield displacement, taken as the deformation level corresponding to $F_{R,exp}$;
Δ_u – deformation capacity, taken as the maximum deformation level;
φ – displacement ductility coefficients, obtained by the Δ_u/Δ_p ratio.
Based on the methodology mentioned above, the calculation results of these characteristic points for all NS specimens and HSS ones were summarized in Table 5 and Table 6 respectively.

3.3. Initial stiffness of T-stub joints

According to the research results pointed out by Zhu et al. [30], the bolt preloading has little effect on the ultimate bearing capacity of the T-stubs, while it can improve significantly the stiffness of the ones. Two phenomena should be adopted to clarify the effect of bolt preloading on the stiffness for the joints [18]. (1) Bolt preloading causes an increase in the axial stiffness of the system made of the bolt and the connected plates considered as a whole. (2) Bolt preloading modifies the overall behavior of the T-stub affecting both the flange span and its restraining conditions. For instance, Fig. 8 shows the influence of bolt preloading, which can be interpreted by means of two ideal levels of the T-stub axial stiffness. The first level (line a) corresponds to a tightening force equal to zero; the second level is given by the stiffness of the initial branch affected by bolt preloading. The dashed curve (b),

Table 5
Main characteristics values of load-displacement curves of T-stub joints using NS.

Specimen code	K (kN)	R (kN)	$F_{R,exp}$ (kN)	F_{max} (kN)	$k_{e,exp}$ (kN·mm^{-1})	$k_{p\text{-}y,0}$ (kN·mm^{-1})	$k_{e,exp}$ / $k_{p\text{-}y,0}$	Δ_p (mm)	Δ_u (mm)	φ
WT1	97	147	143.29	190.05	67.61	1.661	40.70	2.04	32.94	16.15
WT2	98	162	157.71	220.25	161.50	1.635	98.78	0.92	43.70	47.50
WT3	109	177	163.15	238.93	129.30	2.644	48.90	1.32	41.67	31.57
WT4	96	154	141.39	198.92	99.95	2.686	37.21	1.50	25.70	17.13
WT5	75	190	176.25	267.72	188.10	2.521	74.61	1.04	39.70	38.17
WT6	119	201	192.01	289.50	182.40	3.963	46.03	1.09	41.35	37.94
WT7	81	100	97.73	140.89	51.75	2.218	23.33	1.78	43.64	24.52
WT8	37	66	62.61	–	25.52	0.639	39.94	2.29	–	–
WT9	109	170	163.80	227.35	131.30	2.148	61.13	1.26	34.78	27.60
WT10	107	170	166.06	229.11	189.80	1.952	97.23	0.90	37.90	42.11

corresponding to the second stiffness level, represents the ideal case in which the bolt preloading prevents the detachment of the connected flanges for any given value of the external axial load. Obviously, the actual behavior of the connection lies between the two ideal cases, the axial stiffness relationship of the T-stub joints in different bolt preloading level has been provided by Faella et al. [18].

$$K_\eta = \frac{K_1}{\eta + (1-\eta)\frac{K_1}{K_0}} \tag{2}$$

where K_1 is the secant stiffness with bolt preloading value equal to 80% of bolt yield resistance, and K_0 is the one without bolt preloading; In the intermediate cases, the secant stiffness is K_η, η is the bolt preloading level as shown in Fig. 8.

Regarding to the axial stiffness evaluation, it is a secant value, corresponding to a load level equal to 2/3 times of the plastic resistance $F_{Rd,0}$, suggested by EC3 [12]. Fig. 9 depicted the unloading curves (phase 2 of test procedure in this study) of these joints, which clearly illustrated that, (1) with the evidence of the slope for F–△ curves, a large axial stiffness is initially observed due to the effect of the bolt preloading, while at a certain load level the action of bolt preloading 'disappeared' seemingly, and thereafter the axial stiffness of the connections decreases to the level without the bolt preloading. (2) The axial stiffness level depends on the theoretical elastic limit of the specimens. Fig. 9 shows that the axial stiffness of T-stubs using HSS is generally smaller than that of those joints with NS. For easy discussion, the symbol (′) is employed to distinguish all the mechanical index between HSS and NS specimens. Such as the $k'_{e,exp}$ and $k_{e,exp}$ represent the initial stiffness of the specimens made of HSS and NS respectively. Summary of the comparison the experimental results related to the initial stiffness between HSS and NS T-stubs is presented in Table 7, which also confirms the above statements concerning the initial stiffness evaluation for those joints using HSS and NS. This phenomenon should result from the following two reasons. On one hand, when the elastic limit of T-stubs are controlled by the flange yield, the elastic limit load of the T-stubs using HSS is larger than that of the one using NS, due to a high elastic deformation limit of HSS obtained. Hence, the inequalities can be established (Fig. 9), $k_{e,exp} > k'_{e,exp} > k_0$, where the k_0

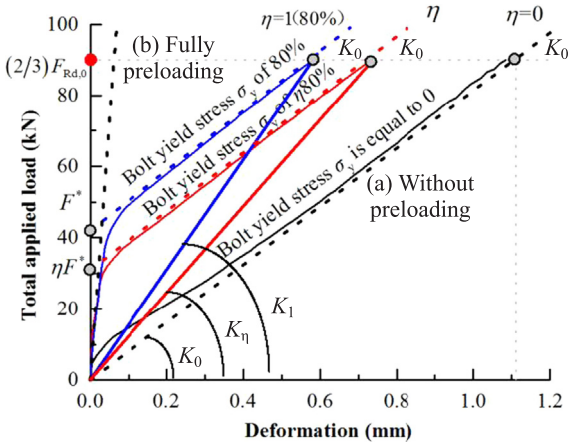

Fig. 8. Interpretation of bolt preloading influence.

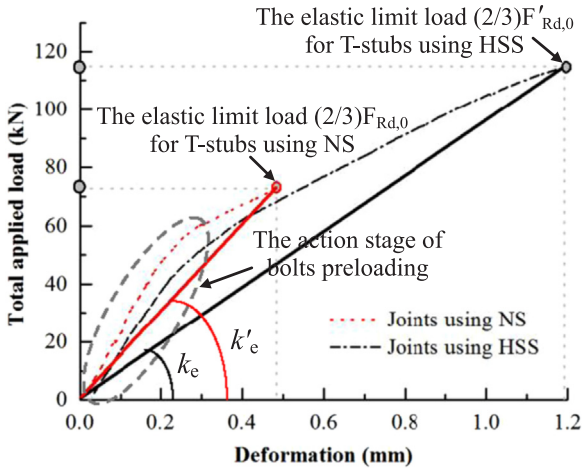

Fig. 9. Initial stiffness under the theoretical elastic limit.

Table 6
Main characteristics values of load-displacement curves of T-stub joints using HSS.

Specimen code	K' (kN)	R' (kN)	$F'_{R,exp}$ (kN)	F'_{max} (kN)	$k'_{e,exp}$ (kN·mm^{-1})	$k'_{p\text{-}y,0}$ (kN·mm^{-1})	$k'_{e,exp}$ / $k'_{p\text{-}y,0}$	Δ'_p (mm)	Δ'_u (mm)	φ'
HWT1	115.71	161.90	152.75	174.67	67.67	9.86	6.86	2.41	4.68	1.94
HWT2	111.84	203.40	201.84	213.42	94.63	1.14	83.01	1.98	12.42	6.27
HWT3	126.46	253.21	230.76	271.49	110.80	2.09	53.01	2.06	18.30	8.88
HWT4	126.30	216.99	202.88	225.19	82.67	1.96	42.18	2.45	20.73	8.46
HWT5	130.20	242.80	241.98	263.25	115.90	1.43	81.05	2.02	17.73	8.78
HWT6	129.72	285.67	267.06	300.44	187.39	3.72	50.37	1.42	14.17	9.98
HWT7	94.16	162.14	160.60	173.16	49.97	0.57	87.67	2.96	25.70	8.68
HWT8	58.59	104.50	104.14	108.26	17.89	0.17	105.24	5.57	42.04	7.55
HWT9	112.07	222.15	211.74	230.71	98.32	3.11	47.50	2.07	28.75	13.89
HWT10	115.41	205.42	205.57	222.25	102.80	2.19	46.94	1.90	15.30	8.05

Table 7
Initial stiffness of T-stub joints.

Specimen code	$k'_{e,exp}$ (kN·mm^{-1}) HWT	$k_{e,exp}$ (kN·mm^{-1}) WT	Relative error (%)
1	67.67	67.61	0.09
2	94.63	161.50	− 41.41
3	110.80	129.30	− 14.31
4	82.67	99.95	− 17.29
5	115.90	188.10	− 38.38
6	187.39	182.40	2.74
7	49.97	51.75	− 3.44
8	17.89	25.52	− 30.00
9	98.32	131.30	− 25.12
10	102.80	189.80	− 45.84

Note that $k'_{e,exp}$ and $k_{e,exp}$ stand for test value of the initial stiffness for these joints using HSS and NS respectively; Relative error (%) = $(k'_{e,exp} - k_{e,exp}) / k_{e,exp} \times 100\%$.

represents the initial stiffness of the T-stubs without bolt preloading. Table 7 shows that the initial stiffness of HSS T-stubs is lower than that of NS ones by about − 3% to − 46%. However, when the elastic limit of T-stubs is governed by bolt strength, the initial stiffness among these joints made of different steel grades is the same due to the identical elastic limit obtained, and thus $k_{e,exp} \approx k'_{e,exp}$, but greater than k_0. As expected, the initial stiffness between HWT1 and WT1 is nearly the same (Table 7), since bolt governed simply collapse in the case.

On the other hand, under the elastic limit cases, the bolt bending effect in the HSS T-stubs should be more significant, leading to relatively weak restraining conditions on the flange when compared to the specimens using NS. If the flange/bolt stiffness ratio is very large, the prying force caused by the flange bending deformation can be ignored, therefore, the bolt bending effect should be small and restraining action can be modeled as simple supports. However, if the opposite cases occur in the ratio, the bolt bending effect should be still small and restraining action can be regarded as fixed supports, for instance, only 3% of the deviations for the initial stiffness is observed in between the specimens HWT6 and WT6 (Table 7). In the intermediate cases, the influence of bolt bending effect on initial stiffness should not be neglected in HSS connections. For example, the initial stiffness of the specimens HWT2, HWT5 and HWT10 is around − 41%, − 38% and − 46% lower than that of the specimens WT2, WT5 and WT10 respectively, which further implied that, to increase the initial stiffness of the connection made of HSS, the larger bolt diameter is needed when compared to the one in the connection with NS.

3.4. Bearing capacity of T-stub joints

Fig. 10 shows the comparison of the bearing capacity for the specimens with HSS and NS, varying with the bolt diameter both grade 8.8 *s* and 10.9 *s*, and the *e*/*d* ratio, the experimental value of which is set out in Table 8. It can be seen from Table 8 that the plastic resistance for T-stubs with HSS is higher than that of the ones using NS by about 24–66%, while merely 7% of increases for plastic resistance is obtained

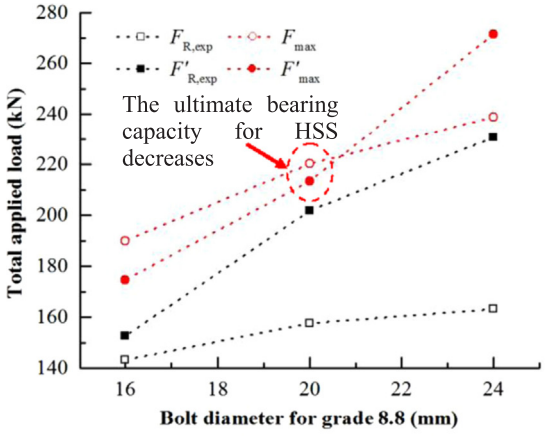

(a) Influence of the grade 8.8*s* bolts

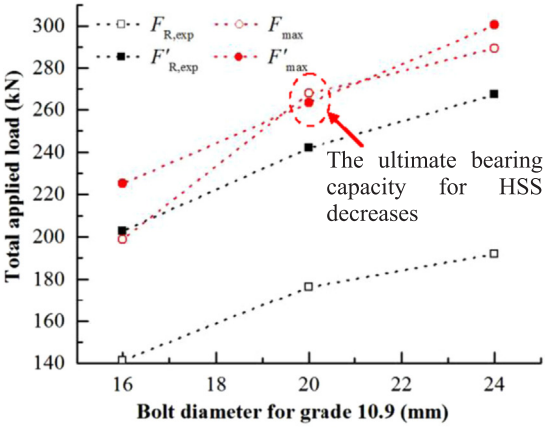

(b) Influence of the grade 10.9*s* bolts

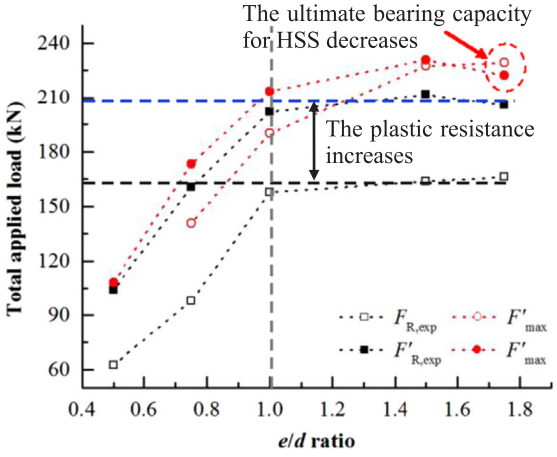

(c) Influence of the *e*/*d* ratio

Fig. 10. Comparison of bearing capacity.

Table 8
Plastic resistance and bearing capacity of T-stub joints.

Specimen code	$F'_{R,exp}$ (kN) HWT	$F_{R,exp}$ (kN) WT	F'_{max} (kN) HWT	F_{max} (kN) WT	Relative error 1 (%)	Relative error 2 (%)
1	152.75	143.29	174.67	190.05	6.60	− 8.09
2	201.84	157.71	213.42	220.25	27.98	− 3.10
3	230.76	163.15	271.49	238.93	41.44	13.63
4	202.88	141.39	225.19	198.92	43.49	13.20
5	241.98	176.25	263.25	267.72	37.29	− 1.67
6	267.06	192.01	300.44	289.50	39.09	3.78
7	160.60	97.73	173.16	140.89	64.33	22.90
8	104.14	62.61	108.26	–	66.33	–
9	211.74	163.80	230.71	227.35	29.27	1.48
10	205.57	166.06	222.25	229.11	23.79	− 2.99

Note that, $F'_{R,exp}$ and $F_{R,exp}$ represent test value of plastic resistance for these joints using HSS and NS respectively, while F'_{max} and F_{max} are test value of ultimate (maximal) bearing capacity for specimens using HSS and NS respectively.
Relative error 1 (%) = $(F'_{R,exp} - F_{R,exp}) / F_{R,exp} \times 100\%$; Relative error 2 (%) = $(F'_{max} - F_{max}) / F_{max} \times 100\%$.

in specimen HWT1 when compared to the specimen WT1, due to prematurely stripping of the nut threads occurred in specimen HWT1. Nevertheless, except for specimen HWT1, a sharp increase of the plastic resistance is observed in between specimens using HSS and NS, since flange fracture or mixed failure governed the ultimate conditions in the remaining specimens. For example, the plastic resistance of specimen HWT8 is about 66% higher than that of the corresponding specimen WT8. However, as shown in Fig. 10c, when the $e/d \geq 1.0$, the plastic resistance will not increase obviously in specimens using NS, and a identical situation was also obtained in specimens with HSS.

The ultimate tensile strength is generally regarded as the safety reserve of materials, which is of great significance to the safety and reliability of structures. It can be seen from Fig. 10 that, not the same as a superior plastic resistance for HSS joints, the ultimate bearing capacity of the welded T-stub joints with HSS is not higher than that of the joints using NS, and even decreases. For instance, Table 8 clearly shows that, the ultimate bearing capacity of the specimens with HSS is slightly higher than that of the corresponding specimens with NS by about 1–23%. Apart from the specimen HWT1 due to the premature bolts failure, the bearing capacity of the specimens HWT2, HWT5 and HWT10 decreased by about − 3%, − 2% and − 3% respectively, in comparison with that of the corresponding specimens with NS. This fact may be attributed to the difference in ductility and ultimate strength to yield strength ratio between HSS and NS. The catenary action can improve significantly ultimate bearing capacity of connections [31], due to the large ductility and the relatively high ultimate strength to yield strength ratio of the NS material, the catenary effect can be fully developed before the fracture of T-stub flange near the weld toe. However, due to limited ductility and the much lower ultimate strength to yield strength ratio of the HSS material, the specimens may have failed at small bending deformations of the flange, before the catenary effect initiated.

3.5. Ductility of T-stubs

Regarding to the ductility evaluation of T-stubs, a component ductility index φ was proposed by da Silva et al. [32], which allows a direct classification of each component in terms of ductility, for instance, adopting the three ductility classes presented by Kuhlmann et al. [33]:

Class 1–components with high ductility ($\varphi > \alpha$).

Class 2–components with limited ductility ($\beta < \varphi \leq \alpha$).

Class 3–components with brittle failure ($\varphi < \beta$).

where α and β represent ductility limits, herein $\alpha = 20$, $\beta = 3$, suggested by da Silva et al. [32].

The experimental values of ductility index for the various tests are listed in Table 9, which compares the ratio between the ductility index

Table 9
Ductility indexes at failure of T-stub joints.

Specimen code	φ' HWT	φ WT	φ'/φ
1	1.94	16.15	0.12
2	6.27	47.50	0.13
3	8.88	31.57	0.28
4	8.46	17.13	0.49
5	8.78	38.17	0.23
6	9.98	37.94	0.26
7	8.68	24.52	0.35
8	7.55	–	–
9	13.89	27.60	0.50
10	8.05	42.11	0.19

φ' and φ denoting ductility indexes of the specimens at failure, using HSS and NS respectively.

of welded T-stubs with HSS and NS. It is clearly shown that for the specimens with NS, apart from the specimens WT1 and WT4 belonging to the components with limited ductility, the remaining specimens are the components with high ductility according to the classification in [32,33]. However, for the specimens using HSS, most of them are the components with limited ductility, expect for the specimen HWT1 belonging to the components with brittle failure. In addition, the ductility index of the welded T-stub joints with HSS is only about 0.12–0.50 t imes of that of the ones using NS, which implies that the ductility of welded T-stub joints using HSS decreases greatly compared to NS welded T-stub joints.

4. Theoretical analysis for T-stub joints with HSS and NS

4.1. Stiffness evaluation of T-stub joints

4.1.1. Faella stiffness formulation

According to the component method, the initial stiffness of a couple of T-elements connected by one bolt row with the identical flange thickness of the upper and lower T-stubs is computed by the following formulation:

$$k_{e,0} = \frac{1}{\frac{2}{k_{e,T}} + \frac{1}{k_{e,b}}} \tag{3}$$

where $k_{e,T}$ and $k_{e,b}$ denote the axial stiffness of the single T-stub element and a bolt row, respectively. Based on an equivalent cantilever, the $k_{e,T}$ is suggested by Faella et al. [34].

$$k_{e,T} = \frac{0.5 E b'_{eff,j} t_f^3}{m^3} \tag{4}$$

where E and t_f represent elastic modulus and flange thickness of the T-

stub element, respectively. It is noted that $b'_{eff,j}$, the effective width, is determined by assuming a 45° spreading of the bolt action starting from the bolt head edge. The axial stiffness of a bolt row is equal to:

$$k_{e,b} = 1.6\frac{EA_b}{L_b} \tag{5}$$

where A_b stands for bolt tensile stress area, and the factor (1.6) approximately accounts for the influence of the prying forces on the axial stiffness of a bolt row, and L_b is the conventional bolt length, defined as follows:

$$L_b = 2t_f + 2t_{wsh} + 0.5(t_n + t_h) \tag{6}$$

where t_{wsh}, t_n and t_h, represent the washer, nut and bolt head thickness, separately.

However, note that the effect of the bolt preloading on the axial stiffness of T-stubs is not incorporated into the method mentioned above. Moreover, based on the experimental and theoretical methods, the axial stiffness of T-stubs with bolt preloading was formulated by Faella et al. [18]. They considered independently two phenomena affecting the axial stiffness for T-stubs. In one case, the bolt preloading leads to an increase of the axial stiffness of the bolt-plate system [34]. The formulation between the pretensioned bolt axial stiffness $k_{e,bp}$ and the nonpretensioned one $k_{e,b}$ is written as

$$\frac{k_{e,bp}}{k_{e,b}} = 4.10 + 3.25\frac{t_f}{d_b} \tag{7}$$

In another case, bolt preloading affects the flexural deformability of flanges for T-stubs, which is fairly dependent on the parameter β expressed as follows accounting for the ratio between the flexural stiffness of the flanges and the bolt axial stiffness.

$$\beta = \frac{t_f}{d_b\sqrt{\alpha}} \tag{8}$$

where the parameter α is m/d_b ratio. Note that according to relative levels of the parameter β, the bolt restraining action can be classified as 'Simple support', 'Fixed support' and the intermediate case 'Semi-fixed support' (see Fig. 11). For the first one ($\beta = \infty$), the axial stiffness of the single T-stub elements can be represented by Eq. (4). Moreover, for the last one ($\beta = 0$), it can be evaluated by the following equation:

$$k_{e,T} = \frac{2Eb'_{eff}t_f^3}{\left(m - \frac{d_h}{2}\right)^3} \tag{9}$$

where d_h denotes bolt head diameter. However, the actual restraining action of the bolts lies in between these two ideal situations. To account both for the parameter β and for the reduction of m due to the bolt head restraining action (see Eq. (9)), therefore a empirical stiffness coefficient ψ is introduced into the Eq. (4), and it can be rewritten as:

$$k_{e,T} = \psi\frac{0.5Eb'_{eff,j}t_f^3}{m^3} \tag{10}$$

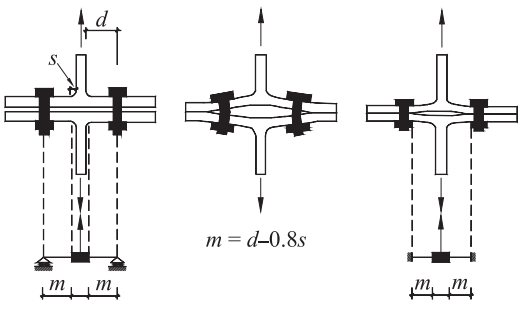

Fig. 11. Behavioral schemes of equivalent T-stub joints.

Based on the research results on T-stubs using Fe430 steel (mild structural steel, nominal yield stress of 275 MPa), and supposing the predicted values of the T-stub stiffness is equal to the experimental ones, the relationship between empirical stiffness coefficient ψ and β is determined by regression analysis, and the expression is given in [18].

$$\psi = 0.57\beta^{-1.28} \tag{11}$$

Furthermore, the influence of the bolt bending effect on the T-stub stiffness is also taken into account by means of the coefficient ψ.

4.1.2. Eurocode 3 formulation

For easy practical design, effect of the bolt preloading on the T-stub stiffness is ignored by Eurocode 3 Part 1–8 [12]. By using the approach, similar to that proposed by Faella et al. [34], to obtain the stiffness of the bolted T-stubs, the initial stiffness of the single T-stub elements may be simplified to the following expressions:

$$k_{e,T} = \frac{Eb'_{eff}t_f^3}{m^3} \tag{12}$$

where b'_{eff}, the effective length, represents a new effective length given in [12], slightly different from $b'_{eff,j}$ mentioned above. By comparing the Eq. (10) and Eq. (12), the empirical stiffness coefficient ψ is taken as 2.0 in EC3, which shows that influence of the bolt restraining action on the T-stub stiffness has been approximately taken into account in EC3. The axial stiffness of a bolt row and of the overall bolted T-stubs were given by Eq. (5) and Eq. (3), respectively.

4.2. Comparing the predicted values with the test results for the initial stiffness

Table 10 displays the predicted values for the initial stiffness and compares them with the experiments. In the range of T-stubs using NS, the predicted values adopted EC3 formulation are about 0.57 – 1.73 times of the test ones, while for Faella stiffness formulation it is around 0.73–1.71 times of the test ones, and a small coefficient of variation is found in the ratio between Faella formulation predicted values and the test ones. The phenomenon shows that the Faella formulation may be more reliable when compared to the EC3 formulation for stiffness prediction. As mentioned above, EC3 formulation approximately accounts for the effect of the coefficient ψ on the T-stub stiffness, simply taken as 2.0, which not fully considers influence of the modification of the type of restraint, varying from the simple support to the fixed restraint, on T-stubs stiffness. Hence, when the flange restraining action is close to these two ideal situations, the differences between the predicted values and test ones, provided by EC3, may be larger when compared to those in the intermediate cases. For instance, the predicted value for specimen WT1 is 73% higher than the test value, and for specimen WT8 is 43% lower than the test one, near the simple support and fixed restraint respectively. However, both in these two ideal cases,

Table 10
Comparison of the calculated and test results for initial stiffness.

Specimen code	$k_{e,0}$ / $k_{e,exp}$ WT	$k_{e,j}$ / $k_{e,exp}$ WT	$k_{e,0}$ / $k'_{e,exp}$ HWT	$k_{e,j}$ / $k'_{e,exp}$ HWT
1	1.73	1.71	1.86	1.90
2	0.73	0.80	1.34	1.55
3	1.27	1.46	1.18	1.51
4	1.24	1.22	1.51	1.55
5	0.71	0.77	1.15	1.31
6	0.74	0.89	0.69	0.89
7	1.11	1.41	0.95	1.32
8	0.57	0.96	0.70	1.27
9	0.96	1.06	1.24	1.27
10	0.67	0.73	1.25	1.44

$k_{e,0}$ and $k_{e,j}$ denote the initial stiffness predicted by EC3 and Faella mode respectively.

by using Faella formulation, the predicted value of specimen WT1 is 71% higher than the test one, while only 4% of the deviations is obtained in between the predicted and test one for the specimen WT8, which implied that the Faella stiffness formulation is effective when the flange restraints are near fixed supports and intermediate case, and while near the simple supports, it should be further calibrated. In addition, it should be noted that the simple cases may be unlikely to occur in commonly-used joints, herein only used to compare and analyze the bolt restraining action in the specimens with HSS and NS.

In the range of T-stubs with HSS, it can be easily seen in Table 10 that the theoretical values of initial stiffness predicted by EC3, are around 0.69–1.86 times of the test ones, i.e. obviously, compared with these of the specimens with NS, for the average results, it overestimates this property of the specimens using HSS, this case is just contrary to that of the specimens made of NS (see Table 10). The differences may derive from the fact that the expression as presented in the EC3 stiffness formulation was calibrated for a certain range of joints made of NS. As stated previously, the bolt restraining level for the specimens using HSS is generally lower than that of the corresponding specimens with NS, and thus the initial stiffness of T-stubs with HSS decreases in contrast to that of the corresponding joints with NS. These phenomena can be further illustrated by Faella stiffness formulation, since the type of the bolt restraining action is included in this formulation. For example, through using this formulation, the predicted values for HSS specimens are around 0.89–1.90 times of the test ones. Therefore, in terms of average results of the ratio in Table 10, it shows that, unlike the cases in NS T-stubs, the empirical stiffness coefficient ψ, obtained by the test results of T-stubs using NS, seems not to be applicable to the stiffness prediction of T-stubs with HSS, which significantly overestimates the bolt restraining action of the HSS T-stub joints when compared to the corresponding joints with NS.

4.3. Plastic resistance evaluation

To assess the plastic resistance of the T-stubs, three possible failure modes was defined by EC3 [12], (1) complete yielding of flanges; (2) bolt failure with flange yielding; (3) only bolt failure, as shown in Fig. 12.

Concerning plastic resistance under the complete yielding of flanges (Type-1) evaluation, two methods based on the yield line analysis are provided, as specified by EC3.

$$\text{Method 1: } F_{1,\mathrm{Rd},0} = \frac{4M_{\mathrm{f,Rd}}}{m} \tag{13}$$

$$\text{Method 2: } F_{1,\mathrm{Rd},0} = \frac{(32n - 2d_{\mathrm{w}})M_{\mathrm{f,Rd}}}{8mn - d_{\mathrm{w}}(m+n)} \tag{14}$$

The difference between them is that, in method 1 the force due to a bolt is assumed to concentrate on the center line of the bolt. However, the method 2 considers influence of the bolt action on a finite contact area, which leads to a significant increase in resistance, but it is more realistic. In Eqs. (13) and (14), $M_{\mathrm{f,Rd}}$ denotes the plastic flexural resistance of the T-flanges, and is given by:

$$M_{\mathrm{f,Rd}} = \frac{1}{4}t_{\mathrm{f}}^2 f_{\mathrm{y}} b_{\mathrm{eff}} \tag{15}$$

b_{eff} is effective width of the T-flanges for resistance calculations; m and n are geometrical parameters as mentioned in Section 2; d_{w} is diameter of the washer, bolt head, or nut, as appropriate.

In the case of bolt failure with flange yielding (Type-2), the plastic resistance of T-stubs has been obtained:

$$F_{2,\mathrm{Rd},0} = \frac{2M_{\mathrm{f,Rd}}}{m}\left[1 + \frac{(2-\beta_{\mathrm{Rd}})\lambda}{\beta_{\mathrm{Rd}}(1+\lambda)}\right] \tag{16}$$

In addition, for the case only bolt failure (Type-3), its resistance is as follows:

$$F_{3,\mathrm{Rd},0} = 2B_{\mathrm{Rd}} \tag{17}$$

where $\beta_{\mathrm{Rd}} = 2M_{\mathrm{f,Rd}}/B_{\mathrm{Rd}}{\cdot}m$, is the β–ratio, controlling the occurrence of a given failure mode (Fig. 12); the parameter λ is equal to n/m; $B_{\mathrm{Rd}} = 0.9A_{\mathrm{b}}f_{\mathrm{u,b}}$, represents the plastic resistance of a single bolt in tension [12]. Eventually, the plastic resistance of the T-stubs is computed as the smallest value among three possible failure modes presented above, i.e. $F_{\mathrm{Rd},0} = \min\{F_{1,\mathrm{Rd},0}, F_{2,\mathrm{Rd},0}, F_{3,\mathrm{Rd},0}\}$.

4.4. Comparison of the predicted values with the test results for the plastic resistance

Tables 11 and 12 demonstrate the Eurocode 3 [12] predictions and the plastic resistances of the tests for the specimens using NS and HSS respectively. Herein the specimen HWT1 with premature stripping of the nut thread was excluded in this discussion, since its plastic resistance is lower than the normal one. It can be clearly seen in Table 11 that, compared with the EC3 equation predictions, the test results of the specimens with NS can be predicted conservatively. For instance, using the nominal yield strength of the NS material, the test results of the specimens with NS is higher than $F_{\mathrm{Rd},1}$ combination by about 37–103%. Even using $F_{\mathrm{Rd},2}$ combination, it is still up to about 22–64% higher than the prediction values. Adopting the actual yield strength of the NS material, those of the specimens with NS are about 13–68% and 0.5–35% higher than $F_{\mathrm{Rd},1}$ combination and $F_{\mathrm{Rd},2}$ combination respectively. Moreover, note that the test results of the NS specimens are all higher than these predicted by the EC3 equations, and thus it is safe for the prediction of plastic resistance of specimens using NS in practice. However, Table 12 shows that the predicted results from the EC3 equations for the specimens with HSS are not so conservative when compared to the test results. For example, employing the nominal one of the HSS material, the test results of the specimens using HSS is around 22–64% and 5–31% more than the $F_{\mathrm{Rd},1}$ combination and $F_{\mathrm{Rd},2}$ combination respectively. When the actual one of the HSS material is adopted in EC3 resistance equations, it seems to be able to well predict the test results of the specimens using HSS: 9–44% higher than the $F_{\mathrm{Rd},1}$ combination and only 3–15% more than the $F_{\mathrm{Rd},2}$ combination, while some overestimated phenomena obtained by EC3 equations are

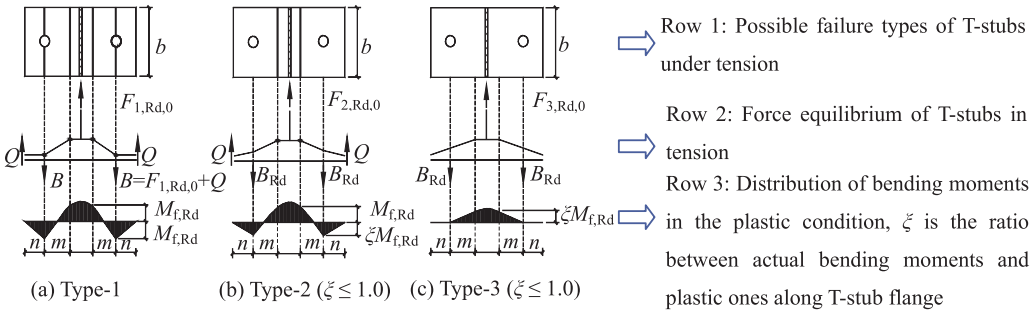

Fig. 12. T-stub failure modes.

Table 11
Comparison of the calculated and test results for plastic resistance of the studied T-stub joints using NS.

Specimen code	$F_{R,exp}$(kN)	EC3 Eqs. (kN) Nominal (Actual)		Failure mode	Relative error 1 (%)	Relative error 2 (%)
		$F_{Rd,1}$	$F_{Rd,2}$			
WT1	143.29	90.45 (109.48)	101.41 (122.75)	Mixed mode	58.42 (30.88)	41.30 (16.73)
WT2	157.71	90.84 (109.95)	105.19 (127.32)	Flange fracture	73.61 (43.44)	49.93 (23.87)
WT3	163.15	102.47 (124.03)	124.47 (150.66)	Flange fracture	59.22 (31.54)	31.08 (8.29)
WT4	141.39	93.31 (112.94)	106.54 (128.96)	Mixed mode	51.53 (25.19)	32.71 (9.64)
WT5	176.25	94.89 (114.86)	112.51 (136.19)	Weld fracture	85.74 (53.45)	56.65 (29.41)
WT6	192.01	94.68 (114.61)	117.44 (142.15)	Flange fracture	102.80 (67.53)	63.50 (35.08)
WT7	97.73	71.24 (86.25)	80.36 (97.27)	Weld fracture	37.18 (13.31)	21.62 (0.47)
WT8	62.61	44.22 (53.53)	48.49 (58.69)	–	41.59 (16.96)	29.12 (6.68)
WT9	163.80	93.96 (113.74)	108.53 (131.37)	Stripping of the nut thread	74.33 (44.01)	50.93 (24.69)
WT10	166.06	93.70 (113.42)	108.28 (131.07)	Mixed mode	77.23 (46.41)	53.36 (26.70)

For EC3 Eqs. results, the nominal series denote results obtained by using nominal yield strengths of f_y = 345 MPa for the Q345 steel; while the actual series denote results obtained by using actual yield strengths of f_y = 417.6 MPa for the Q345 steel. $F_{Rd,1}$ = min{Eq. (13), Eq. (16), Eq. (17)}; $F_{Rd,2}$ = min{Eq. (14), Eq. (16), Eq. (17)}; Relative error 1 (%) = $(F_{R,exp}-F_{Rd,1})/F_{Rd,1}$ × 100%; Relative error 2 (%) = $(F_{R,exp}-F_{Rd,2})/F_{Rd,2}$ × 100%.

observed in the specimens with HSS: the test results of the specimens HWT2, HWT9 and HWT10 are lower than the predicted ones by about − 6%, − 2% and − 5% respectively, which implies that the EC3 resistance equations may be not safe to predict the actual resistance of the welded T-stubs with HSS. The differences may derive from the post-welding properties in the specimens with HSS and NS, the local softening effect will be inevitably introduced near the weld toe in the welding. For the specimens using NS, some research results suggest that if the width of the soft zone does not exceed 25% of the plate thickness, local softening would not necessarily impair the global strength due to the constraints of the stronger weld metal and unaffected base metal [14,35,36], while such assumption may not be applied to the welded T-stub joints using HSS. The tensile test of the post-welding HSS specimens with butt weld was conducted in [37], and the steel materials are the same as these studied herein, and their research results showed that, all post-welding specimens with Q690 steel failed in the heat affected zone (HAZ), where the soft zone also occurred, the 0.2% proof stress and the ultimate tensile stress are, at average, lower than those of base metal by about 26% and 10% respectively, the average hardness in HAZ is lower than base metal by about 14%. While for the specimens using Q345 steel, failed in the HAZ, the 0.2% proof stress and the ultimate tensile stress are, at average, higher than those of base metal by only 1.7–5.1% and 4.4–6.5%, the average hardness in HAZ was slightly lower than base metal by 5.2%. All of which implies that the mechanical properties of post-welding specimens with HSS will deteriorate significantly, especially for the strength. The plastic resistance of the bolted T-stubs is too much dependent on the flange/bolt strength ratio. For the specimens with HSS, in Table 12 except the specimens HWT1 and HWT4 failed in bolt fracture, the remaining specimens using HSS occur in flange fracture near the weld toe, and thus plastic resistance of those specimens may be lower than the actual one, due to the effect of welding process. This conclusion may be able to support the fact that the actual plastic resistance of welded T-stubs using HSS is overestimated by EC3 equations.

5. Conclusions

The research work covered all possible failure modes and highlighted the differences in mechanical property of the welded T-stub joint with Q690 HSS and Q345 NS under bolt preloading cases, varying with the bolt type and the flange geometry. In the experimental study phase, the failure mode, load-displacement behavior, initial stiffness, plastic resistance, ultimate bearing capacity and ductility index of the welded T-stubs with HSS and NS were qualitatively and quantitatively evaluated. In the theoretical study phase, the stiffness formulations proposed by Faella et al., the stiffness and the plastic resistance equations suggested by the EC3 Part 1–8 were also further validated against the experimental results. The following conclusions can be drawn from the experimental and theoretical study:

(1) The failure mode of the welded T-stub joints using HSS is basically the same as that of those joints with NS. Fracture of the bolts or the welds presents a brittle rupture mode, and the failure of only the flange occurred near the weld toe can ensure a good ductility for the welded T-stub joints with NS, but for HSS welded T-stub joints there is still a brittle rupture mode due to little necking developed.
(2) When the elastic limit of T-stubs is governed by the flange yield, the flange restraining level for the T-stub joints using HSS is generally

Table 12
Comparison of the calculated and test results for plastic resistance of the studied T-stub joints using HSS.

Specimen code	$F'_{R,exp}$ (kN)	EC3 Eqs. (kN) Nominal (Actual)		Failure mode	Relative error 1 (%)	Relative error 2 (%)
		$F'_{Rd,1}$	$F'_{Rd,2}$			
HWT1	152.75	145.77 (166.13)	145.77 (166.13)	Stripping of the nut thread	*4.79* (*−8.05*)	*4.78* (*−8.05*)
HWT2	201.84	162.14 (184.78)	188.81 (215.58)	Flange fracture	24.49 (9.23)	6.90 (**−6.37**)
HWT3	230.76	163.05 (185.82)	197.34 (224.90)	Flange fracture	41.53 (24.18)	16.94 (2.61)
HWT4	202.88	163.05 (185.82)	172.93 (197.08)	Mixed mode	24.43 (9.18)	17.32 (2.94)
HWT5	241.98	163.05 (185.82)	194.24 (221.36)	Flange fracture	48.41 (30.22)	24.58 (9.32)
HWT6	267.06	163.05 (185.82)	203.41 (231.81)	Flange fracture	63.79 (43.72)	31.29 (15.21)
HWT7	160.60	119.07 (131.31)	134.32 (148.13)	Flange fracture	34.88 (22.31)	19.57 (8.42)
HWT8	104.14	75.86 (83.66)	83.14 (91.69)	Flange fracture	37.28 (24.48)	25.26 (13.58)
HWT9	211.74	168.50 (185.82)	196.71 (216.93)	Flange fracture	25.66 (13.95)	7.64 (**−2.39**)
HWT10	205.57	168.50 (185.82)	196.45 (216.65)	Flange fracture	22.00 (10.63)	4.64 (**−5.11**)

For EC3 Eqs. results, the nominal series denote results obtained by using nominal yield strengths of f_y = 690 MPa for the Q690 steel; while the actual series denote results obtained by using actual yield strengths of f_y = 760.9 MPa for the Q690 steel. $F_{Rd,1}$ = min{Eq. (13), Eq. (16), Eq. (17)}; $F_{Rd,2}$ = min{Eq. (14), Eq. (16), Eq. (17)}; Relative error 1 (%) = $(F_{R,exp}-F_{Rd,1})/F_{Rd,1}$ × 100%; Relative error 2 (%) = $(F_{R,exp}-F_{Rd,2})/F_{Rd,2}$ × 100%.

lower than that of the corresponding joints with NS in the elastic limit, and thus the initial stiffness of T-stubs with HSS decreases in contrast to that of the corresponding joints with NS. However, when the elastic limit of T-stubs is controlled only by the bolt strength, the initial stiffness among these joints made of different steel grades is the same due to the identical elastic limit obtained.

(3) The plastic resistance of welded T-stubs with HSS is higher than that of those joints using NS by about 24–66%, while its ultimate bearing capacity is slightly more than that of those joints with NS by about 1–23%, because of the poor ductility and plastic deformability of the HSS material. The ductility index of the welded T-stub joints with HSS is only about 0.12 – 0.50 times of that of the ones using NS.

(4) The coefficient ψ in Faella stiffness formulations, obtained by the test results of T-stubs using NS, seems not to be applicable to the stiffness prediction of welded T-stubs with HSS, which significantly overestimates the bolt restraining action of HSS T-stub joints when compared to the corresponding joints with NS.

(5) EC3 resistance equations may be not safe to predict the actual resistance of the welded T-stub joints with HSS when the flange fracture near the weld toe governs the collapse, due to the effect of welding process.

Acknowledgements

The financial support by the National Natural Science Foundation of China No. 51308454 and the China Postdoctoral Science Foundation No. 2013M542371 are much appreciated.

References

[1] J. Raoul, H.P. Günther, Use and Application of High-performance Steels For Steel Structures, Zürich, IABSE-AIPC-IVBH, Switzerland, 2005.
[2] R. Bjorhovde, Development and use of high performance steel, J. Constr. Steel Res. 60 (3–5) (2004) 393–400.
[3] R. Bjorhovde, Performance and design issues for high strength steel in structures, Adv. Struct. Eng. 13 (3) (2010) 403–411.
[4] G. Haaijer, Economy of high strength steel structural members, J. Struct. Div. (ASCE) 87 (8) (1961) 1–23.
[5] Y.B. Wang, G.Q. Li, S.W. Chen, F.F. Sun, Experimental and numerical study on the behavior of axially compressed high strength steel box-columns, Eng. Struct. 58 (2014) 79–91.
[6] P. Langenberg, Relation between design safety and Y/T ratio in application of welded high strength structural steel, in: Proceedings of International Symposium on Application of High Strength Steels in Modern Constructions and Bridges Rationship of Design Specifications, Safety and Y/T Ratio, Beijing, China, 2008, pp. 28–46.
[7] F.F. Sun, M. Sun, G.Q. Li, Y. Xiao, M. Wei, L.X. Liu, Experimental study on seismic behavior of high-strength steel beam-to-column end-plate connections, J. Build. Struct. 35 (4) (2014) 116–124 (in Chinese).
[8] A.M. Girão Coelho, F.S.K. Bijlaard, Experimental behavior of high strength steel endplate connections, J. Constr. Steel Res. 63 (9) (2007) 1228–1240.
[9] X.H. Qiang, X. Jiang, F.S.K. Bijlaard, H. Kolstein, Y.F. Luo, Behaviour of beam-to-column high strength steel endplate connections under fire conditions – Part 1: experimental study, Eng. Struct. 64 (2014) 23–38.
[10] X.H. Qiang, X. Jiang, F.S.K. Bijlaard, H. Kolstein, Y.F. Luo, Behaviour of beam-to-column high strength steel endplate connections under fire conditions – Part 2: numerical study, Eng. Struct. 64 (2014) 39–51.
[11] S. Jordão, L. Simões da Silva, R. Simões, Design formulation analysis for high strength steel welded beam-to-column joints, Eng. Struct. 70 (2014) 63–81.
[12] EN 1993-1-8, Eurocode 3: Design of Steel Structures Part 1–8: Design of Joints, European Committee for Standardization, Brussels, 2005.
[13] M.S. Zhao, C.K. Lee, S.P. Chiew, Tensile behavior of high performance structural steel T-stub joints, J. Constr. Steel Res. 122 (2016) 316–325.
[14] M.S. Zhao, C.K. Lee, T.C. Fung, S.P. Chiew, Impact of welding on the strength of high performance steel T-stub joints, J. Constr. Steel Res. 131 (2017) 110–121.
[15] C. Chen, X. Zhang, M. Zhao, C.K. Lee, T.C. Fung, S.P. Chiew, Effects of welding on the tensile performance of high strength steel T-stub joints, Structure 9 (2017) 70–78.
[16] J.W.B. Stark, Criteria for the use of preloaded bolts in structural joints, Connect. Steel Struct. III (1996) 431–440.
[17] G.L. Kulak, High Strength Bolting for Canadian Engineers, Canadian Institute for Steel Construction, Quadratone Graphics Ltd, Toronto, 2005.
[18] C. Faella, V. Piluso, G. Rizzano, Experimental analysis of bolted connections: snug versus preloaded bolts, J. Struct. Eng. 124 (7) (1998) 765–774.
[19] G. Liang, H.C. Guo, Y.H. Liu, Y.L. Li, Q690 high strength steel T-stub tensile behavior: experimental and numerical analysis, Thin-Walled Struct. 122 (2018) 554–571.
[20] H.C. Guo, G. Liang, Y.L. Li, Y.H. Liu, Q690 high strength steel T-stub tensile behavior: experimental research and theoretical analysis, J. Constr. Steel Res. 139 (2017) 473–483.
[21] A.M. Girão Coelho, F.S.K. Bijlaard, N. Gresnigt, L. Simões da Silva, Experimental assessment of the behaviour of bolted T-stub connections made up of welded plates, J. Constr. Steel Res. 60 (2004) 269–311.
[22] EN 1993-1-12, Eurocode 3: Design of Steel Structures, Part 1–12: General: High Strength Steels, European Committee for Standardization, Brussels, 2007.
[23] GB 50661-2011, Code for Welding of Steel Structures, China Architecture & Building Press, Beijing, 2012 (in Chinese).
[24] EN 1993-1-1, Eurocode 3: Design of Steel Structures: Part 1-1: General Rules and Rules for Buildings, British Standards Institution, London, 2005.
[25] GB/T228-2010, Metallic materials—Tensile testing—Part 1: Method of Test at Room Temperature, China Standard Press, Beijing, 2002 (in Chinese).
[26] GB/T 2975-1998, Steel and Steel Products: Location and Preparation of Test Pieces for Mechanical Testing, China Standard Press, Beijing, 1998 (in Chinese).
[27] A.M. Girão Coelho, Characterization of the Ductility of Bolted End Plate Beam-to-Column Steel Connections (Ph.D. thesis), University of Coimbra, Coimbra, Portugal, 2004.
[28] JGJ82-2011, Technical Specification for High Strength Bolt Connections of Steel Structures, China Standard Press, Beijing, 2011 (in Chinese).
[29] D. Skejic, D. Dujmovic, D. Beg, Behaviour of stiffened flange cleat joints, J. Constr. Steel Res. 103 (12) (2014) 61–76.
[30] X.L. Zhu, P.J. Wang, M. Liu, W.L. Tuoya, S.Q. Hu, Behaviors of one-side bolted T-stub through thread holes under tension strengthened with backing plate, J. Constr. Steel Res. 134 (2017) 53–65.
[31] L. Li, W. Wang, Y.Y. Chen, Y. Lu, Effect of beam web bolt arrangement on catenary behaviour of moment connections, J. Constr. Steel Res. 104 (2015) 22–36.
[32] L.S. da Silva, A. Santiago, P.V. Real, Post-limit stiffness and ductility of end-plate beam-to-column steel joints, Comput. Struct. 80 (2002) 515–531.
[33] U. Kuhlmann, J.B. Davison, M. Kattner, Structural systems and rotation capacity, in: Proceedings of the International Conference on Control of the Semi-Rigid Behaviour of Civil Engineering Structural Connections, Liège, Belgium, 1998, pp. 167–176.
[34] C. Faella, V. Piluso, G. Rizzano, Some proposals to improve EC3-Annex 1 approach for predicting the moment-rotation curve of extended plate connections, Costr. Met. 4 (1996) 15–31.
[35] B. de Meester, The weldability of modern structural TMCP steels, ISIJ Int. 37 (1997) 537–551.
[36] F. Hochhauser, W. Ernst, R. Rauch, R. Vallant, N. Enzinger, Influence of the soft zone on the strength of welded modern HSLA steels, Weld. World 56 (2012) 77–85.
[37] H.C. Guo, L.P. Hao, Y.L. Li, Y.H. Liu, G. Liang, Experimental study on tensile test of butt weld of high strength steel, Chin. J. Appl. Mech. 35 (1) (2018) 172–177 (in Chinese).